

ARTICLE

Population pharmacokinetics of liposomal irinotecan in patients with cancer and exposure–safety analyses in patients with metastatic pancreatic cancer

Karl Brendel¹ | Tanios Bekaii-Saab² | Patrick M Boland³ | Farshid Dayyani⁴ | Andrew Dean⁵ | Teresa Macarulla⁶ | Fiona Maxwell⁷ | Kabir Mody⁸ | Anna Pedret-Dunn⁷ | Zev A Wainberg⁹ | Bin Zhang¹⁰

¹Ipsen, Les-Ulis, France

²Mayo Clinic, Phoenix, Arizona, USA

³Roswell Park Cancer Institute, Buffalo, New York, USA

⁴University of California Irvine, Orange, California, USA

⁵St John of God Hospital Subiaco, Perth, Western Australia, Australia

⁶Vall d'Hebrón University Hospital, Vall d'Hebrón Institute of Oncology, Barcelona, Spain

⁷Ipsen, Abingdon, UK

⁸Mayo Clinic, Jacksonville, Florida, USA

⁹Ronald Regan UCLA Medical Center, Los Angeles, California, USA

¹⁰Ipsen, Cambridge, Massachusetts, USA

Correspondence

Karl Brendel, Ipsen Innovation, ZI de Coutaboëuf, 5 avenue du Canada, 91940 Les-Ulis, France.
Email: karl.brendel@ipsen.com

Abstract

Liposomal irinotecan is a liposomal formulation of irinotecan, which prolongs circulation of irinotecan and its active metabolite SN-38. A population pharmacokinetic (PK) model was developed based on data from seven studies ($N = 440$). Adequacy of the model was assessed using multiple methods, including visual predictive check. Associations between PK exposure and the incidence of diarrhea (grade ≥ 3) and neutropenia adverse events (AEs) (grade ≥ 3) at first event in patients with metastatic pancreatic ductal adenocarcinoma (mPDAC) were investigated using logistic regression based on data from two studies (the phase III NAPOLI-1 [$N = 260$] and phase I/II NCT02551991 [$N = 56$] trials). The PKs of total irinotecan was described by a two-compartment model with first-order elimination, with SN-38 formed directly by a first-order constant from the central compartment of irinotecan or after using a transit compartment. Clearance was 17.9 L/week (0.107 L/h) and 19,800 L/week (118 L/h) for total irinotecan and SN-38, respectively. The UGT1A1*28 7/7 homozygous genotype had no significant impact on SN-38 clearance. Model evaluation was satisfactory for both irinotecan and SN-38. The incidence of diarrhea (grade ≥ 3) at first event was significantly higher with increasing average concentrations of total irinotecan and SN-38; there was no significant association between an increased risk of neutropenia AEs (grade ≥ 3) at first event and average SN-38 concentrations. In summary, the PKs of total irinotecan and SN-38 after administration of liposomal irinotecan were well-described by the model. The UGT1A1*28 status had no significant impact on the PKs of liposomal irinotecan.

Study Highlights

WHAT IS THE CURRENT KNOWLEDGE ON THE TOPIC?

Liposomal encapsulation prolongs the circulation of irinotecan and its active metabolite SN-38, and previous population pharmacokinetic (PK) analyses have

This is an open access article under the terms of the Creative Commons Attribution-NonCommercial License, which permits use, distribution and reproduction in any medium, provided the original work is properly cited and is not used for commercial purposes.

© 2021 The Authors. *CPT: Pharmacometrics & Systems Pharmacology* published by Wiley Periodicals LLC on behalf of American Society for Clinical Pharmacology and Therapeutics.

identified the main covariates affecting the PK profile. Irinotecan and SN-38 were characterized by two independent population PK models with the assumption of encapsulated and unencapsulated SN-38 based on in vitro data for the metabolite.

WHAT QUESTION DID THIS STUDY ADDRESS?

This study aimed to improve characterization of liposomal irinotecan PKs by developing a joint parent-metabolite model in 440 patients and identify covariates (including, for the first time, oxaliplatin co-administration) that affect total irinotecan (encapsulated and unencapsulated) and SN-38 exposure. The associations between estimated PK exposure metrics and key safety endpoints (grade ≥ 3 diarrhea and neutropenia adverse events [AEs]) in patients with metastatic pancreatic ductal adenocarcinoma (mPDAC) were also investigated.

WHAT DOES THIS STUDY ADD TO OUR KNOWLEDGE?

This study confirms that UGT1A1*28 status had no significant impact on the PKs of liposomal irinotecan. In patients with mPDAC (first line or second line), there were significant associations between total irinotecan and SN-38 exposure and diarrhea (grade ≥ 3), but not between SN-38 exposure and neutropenia AEs (grade ≥ 3). Oxaliplatin co-administration seems to have an impact on both total irinotecan and SN-38 exposures.

HOW MIGHT THIS CHANGE DRUG DISCOVERY, DEVELOPMENT, AND/OR THERAPEUTICS?

There is insufficient evidence to suggest a need for dose adjustments of liposomal irinotecan based on UGT1A1*28 genotype, similar to low doses of non-liposomal irinotecan.

INTRODUCTION

Worldwide, pancreatic cancer is the seventh most common cause of cancer-related death and remains an exception to the general trend for improvements in cancer-related mortality.^{1,2} Current recommendations for the first-line (1L) treatment of metastatic pancreatic cancer include gemcitabine-based therapy and, more recently, the FOLFIRINOX regimen (5-fluorouracil [5-FU]/folinic acid [leucovorin (LV)]/irinotecan/oxaliplatin).^{3,4}

Liposomal irinotecan (ONIVYDE; historical names include nal-IRI, MM-398, and PEP02), in combination with 5-FU/LV, is a recommended treatment option for patients with metastatic pancreatic ductal adenocarcinoma (mPDAC) following progression with gemcitabine-based therapy, based on the results of the phase III NAPOLI-1 trial.^{4,5} The active drug, irinotecan, and its metabolite, SN-38, which is 100- to 1000-fold more active than irinotecan, bind reversibly to the topoisomerase 1 DNA complex and prevent religation of the single-strand breaks, causing double-strand DNA damage and preventing replication, thereby arresting uncontrolled cell growth.⁶⁻⁸ SN-38 is cleared via glucuronidation in the liver, primarily by the enzyme uridine diphosphate glucuronosyltransferase 1A1 (UGT1A1), and then by biliary excretion.^{6,7} Studies in patients treated with non-liposomal irinotecan suggest that UGT1A1*28 7/7 homozygosity (prevalence, 13% and 5% in the White and Asian

populations, respectively⁹) is associated with increased SN-38 concentrations, which are linked to higher incidence of hematological toxicity than other genotypes, and that these associations are dose-dependent.¹⁰⁻¹³

With liposomal irinotecan, a lipid bilayer vesicle encapsulates irinotecan, protecting it from hydrolysis and rapid metabolic conversion, leading to prolonged systemic circulation.¹⁴ In a re-analysis of data from a phase II trial in patients with gastric cancer, the geometric mean irinotecan maximum plasma concentration (C_{max}), area under the plasma concentration-time curve (AUC), and half-life were 13.4, 46.2, and two times higher, respectively, with liposomal irinotecan 100 mg/m² free base (120 mg/m² irinotecan hydrochloride trihydrate) every 3 weeks compared with non-liposomal irinotecan 260 mg/m² free base (300 mg/m² irinotecan hydrochloride trihydrate) every 3 weeks.¹⁵ The liposomal formulation also facilitates targeted delivery of the drug to solid tumors. In mouse pancreatic tumor models, liposomal irinotecan improved delivery of the active drug to tumors, compared with non-liposomal irinotecan, and was taken up by tumor-resident macrophages and tumor/stromal cells and locally converted to SN-38.^{16,17} Furthermore, DNA damage was mostly observed in tumor cells, including those outside of the liposomal deposition area, with only minimal DNA damage and apoptosis in non-tumor cells.^{16,17}

In the phase III trial, NAPOLI-1 (NCT01494506), liposomal irinotecan + 5-FU/LV significantly increased both

median overall survival and progression-free survival compared with 5-FU/LV alone in patients with mPDAC that had progressed after previous gemcitabine-based therapy.^{18,19} The most common treatment-emergent adverse events (AEs) of grade 3 or greater liposomal irinotecan + 5-FU/LV in the final analysis of NAPOLI-1 were neutropenia (32%, which also included decreased neutrophil count, neutropenic sepsis, and febrile neutropenia), fatigue (14%), diarrhea (13%), and vomiting (12%).¹⁹ One-year follow-up data from a phase I/II dose-exploration and dose-expansion trial (NCT02551991) of 1L liposomal irinotecan + 5-FU/LV + oxaliplatin in patients with mPDAC who had not previously received treatment in the advanced/metastatic setting showed that treatment-emergent AEs of grade 3 or greater were reported in 22 of 32 patients (68.8%), with neutropenia being the most common (31.3%).²⁰

A population pharmacokinetic (PK) model was previously developed in order to describe the PKs of liposomal irinotecan and SN-38 independently and to assess associations between derived PK parameters and safety outcomes.¹⁵ In the present study, this model was re-assessed by jointly analyzing concentrations of total irinotecan (encapsulated and unencapsulated) and SN-38 with the inclusion of data from the phase I/II 1L mPDAC dose-exploration and dose-expansion trial. The associations between post hoc estimated PK exposure metrics and key safety endpoints (grade ≥ 3 diarrhea and grade ≥ 3 neutropenia AEs at first event) in the NAPOLI-1 and phase I/II 1L mPDAC trials were also investigated.

METHODS

Study data

The population PK analysis was based on data from seven clinical trials, including the phase III NAPOLI-1 trial (NCT01494506), the phase I/II 1L mPDAC study (NCT02551991), and five phase I/II studies in patients with solid tumors (PEP0201, NCT02884128, NCT00813072, NCT00940758, and NCT01770353; Table 1). The design, patient population, and results for each of these studies have been described previously.^{6,19–25} The exposure–safety analyses were based on a subset of data focused on patients with mPDAC from the NAPOLI-1 trial and the phase I/II 1L mPDAC study.

The timing and frequency of PK sampling varied among the seven studies, with samples collected at between four and 13 time points, and up to 8 or 15 days postdose or at end of treatment (Table 1). Plasma samples were analyzed to determine concentrations of total (encapsulated and unencapsulated) irinotecan and SN-38 using validated, specific, and sensitive liquid chromatography–mass spectrometry

methods, with lower limits of quantification (LLOQs) varying between analytes and within and across studies (0.002–1 $\mu\text{g}/\text{mL}$ for irinotecan and 0.441–1 ng/mL for SN-38).

Data management procedures were performed using SAS (version 9.4; SAS-Institute) and R (versions 3.5.2 and 3.5.3; R Development Core team, Foundation for Statistical Computing). The population PK analysis data set included full study data from all seven studies and contained both parent (irinotecan) and metabolite (SN-38) plasma concentration data in mass and molar units, patient characteristics, and additional relevant covariates. Patient characteristics and covariates are shown in Table S1. Actual concentrations of total irinotecan, as the free base (molecular weight of 586.678 g/mol), were used.

Population PK model development

Prior to model development, the PK data were explored by visually inspecting the following profiles/plots created using R (version 3.5.3): dose-normalized concentration–time profiles of total irinotecan and SN-38, overall and stratified by study; percentage of data below the LLOQ for each analyte, overall and by study; incidence of categorical covariates (i.e., gender, race, liver metastasis at baseline, UGT1A1*28 genotyping, manufacturing site, and tumor location at baseline) via bar charts, overall and by study; distribution of continuous covariates (i.e., weight, body surface area, age, creatinine clearance, and alanine aminotransferase [ALT], aspartate transaminase [AST], albumin, and bilirubin levels) via histograms, overall and by study; and potential correlations among covariates. Exploratory graphical evaluations of the data were performed to detect outlier observations or individuals, to guide the selection of an initial structural model, and to identify important features to be considered in the development of the base model.

PK data were analyzed using nonlinear mixed effects modeling (NONMEM) software (version 7.4.1; ICON Development Solutions), running under PsN (Perl-speaks-NONMEM) 4.8.1 on a grid of CentOS Linux servers, and the Intel Fortran compiler, version 12.0.4 (Intel Corporation). Graphical analysis was performed using R.

PK parameters for total irinotecan and SN-38 following liposomal irinotecan administration were estimated jointly using NONMEM. The first-order conditional estimation method with the INTERACTION option was used for all model runs.

Base model

Two- and three-compartment linear disposition models were investigated for total irinotecan, which was assumed

TABLE 1 The seven liposomal irinotecan clinical trials included in the population PK analysis

Study	Phase	Population	N	Liposomal irinotecan dose, mg/m ² . ^a	Concomitant drugs	PK sample collections
PEP0201 ⁶	1	Various tumor types	11	50, 100, or 156 Q3W	None (monotherapy)	Cycle 1: 0 (predose), 0.5, 1.0, 1.5, 2.5, 3.5, 4.5, 7.5, 10.5, 13.5, 25.5, 49.5, 73.5, and 169.5 h after drug infusion. Cycle 2: 0 (predose)
PEP0203 (NCT02884128) ²¹	1	Various tumor types	16	50, 70, 85, or 100 Q3W	5-FU/LV	Cycle 1: 0 (predose), 0.5, 1.0, 1.5, 2.5, 4.5, 10.5, 25.5, 49.5, 73.5, and 169.5 h after drug infusion. Cycle 2: 0 (predose)
PEP0206 (NCT00813072) ²²	2	Various tumor types	37	100 Q3W	None (monotherapy)	Cycle 1: 0 (predose), 0.5, 1.0, 1.5, 2.5, 4.5, 10.5, 25.5, 49.5, 73.5, and 169.5 h after drug infusion. Cycle 2: 0 (predose)
PIST-CRC-01 (NCT00940758) ²³	1	Metastatic colorectal cancer	18	70, 80, 85 Q2W	None (monotherapy)	Cycle 1: 0 (predose), 0.5, 1.0, 1.5, 2.5, 4.5, 10.5, 25.5, 49.5, 73.5, and 169.5 h after drug infusion.
CITS (NCT01770353) ²⁴	1	Various tumor types	42	35, 50, 70 Q2W	None (monotherapy)	Cycle 1 (pilot): 0 (predose), 1.5, 3.0, 72.0, 168.0 and 336.0 h Cycle 2 (expansion): 0 (predose), 1.5, 3.0, 48.0, 168.0 and 336.0 h
NAPOLI-1 (NCT01494506) ^{18,19}	3	mPDAC	260	70 Q2W or 100 Q3W	None (monotherapy) or 5-FU/LV	Cycle 1: 0 (predose), 1.5, 2.5, 48.0 (arm 3 only) and 168.0 h
NCT02551991 ^{20,25}	1/2	mPDAC	56	50, 55, or 70 Q2W	5-FU/LV + oxaliplatin	Cycle 1: 0 (predose), 1.5, 6.0, 48.0, 169.5, 336.0 h and end of treatment

Abbreviations: 5-FU, 5-fluorouracil; LV, leucovorin; mPDAC, metastatic pancreatic ductal adenocarcinoma; PK, pharmacokinetic; Q2W, every 2 weeks; Q3W, every 3 weeks.

^aExpressed as free base.

to be converted into SN-38. One- and two-compartment linear disposition models were investigated for SN-38, with part of irinotecan total elimination clearance forming SN-38. The central volume of distribution of SN-38 had to be assumed equal to the central volume of distribution of irinotecan to prevent identifiability issues. Interindividual variability (IIV) was modeled assuming a log-normal distribution for patient-level random effects (equation is provided in the Supplementary Material).

Residual unexplained variability (RUV) was tested as additive, proportional, or combined (additive + proportional) on the dependent variable (equation for the combined RUV is provided in the Supplementary Material).

Correlations among the IIV of various parameters were also investigated by including additional off-diagonal elements to the OMEGA (Ω) matrix to test correlation between random effects.

For hierarchical (or nested) models, the significance of adding or removing a parameter was assessed using the likelihood ratio test (LRT). For non-nested models, the Akaike information criterion (AIC) and/or the Bayesian information criterion (BIC) were used to compare models following the principle that the lower the AIC and/or BIC, the better the model.

Covariate model building

Covariate analysis was conducted to explain the variability in total irinotecan and SN-38 concentrations. Covariates examined included: the continuous covariates age, body size (body weight, height, body mass index, or body surface area), dose, liver function tests (e.g., ALT, AST, bilirubin, and albumin), and creatinine clearance; and the categorical covariates gender, race, concomitant therapy (i.e., 5-FU/LV and oxaliplatin), and UGT1A1*28 polymorphism. A stepwise covariate model-building approach was applied to the final base joint PK model using an iterative addition and deletion model selection strategy, based on the LRT (p forward = 0.05 and p backward = 0.005).

Continuous covariates were included in the population PK model as power functions, whereas categorical covariates were implemented as factors (equation is provided in the Supplementary Material).

Final model

Following completion of the covariate model building, further model refinements were evaluated. These included evaluation of the residual error structure, assessment of off-diagonal elements of the Ω block to check the need for all included correlations, and a last attempt to account for

data below the LLOQ for both analytes. Initially, below limit of quantification (BLOQ) samples were excluded from the analysis (M1 method). However, there are some instances in which their exclusion can bias PK parameter estimates (e.g., if the proportion of BLOQ samples is high). Therefore, initial models were also evaluated to include BLOQ samples and the likelihood methodology (i.e., "M3"^{26,27}) was used. With the M3 method, the likelihood is maximized for all the data considering different LLOQ values across studies and the BLOQ data are treated as censored. The impact of including the BLOQ samples on the overall goodness-of-fit (visual predictive check [VPC]) and parameter estimates was assessed.

Model evaluation

In accordance with industry guidelines,^{28,29} the performance of the final population PK model was evaluated using several methods, including goodness-of-fit plots, prediction-corrected VPCs (pcVPCs), and uncertainty assessment of PK parameter estimates.^{28–30}

The goodness-of-fit plots comprised: observed concentrations versus population-predicted concentrations and individual-predicted concentrations, with line of identity and trend line; conditional weighted residuals versus population-predicted concentrations, with zero line and trend line; and conditional weighted residuals versus time after dose, with zero line and trend line. Based on the population PK parameter estimates of the final population PK model, time profiles of concentrations of the analytes were simulated in 1000 replicates. Within each bin, 95% prediction intervals of the 2.5th, 50th, and 97.5th percentiles of simulated concentrations were computed across the 1000 replicates and compared with the 2.5th, 50th, and 97.5th percentiles of observed concentrations.

Finally, the robustness of the final population PK model was evaluated by a nonparametric bootstrap procedure. This model evaluation consisted of repeatedly fitting the model to 1000 data sets replicated by randomly sampling individual patient data (including concentration–time data, dosing history, and covariates) with replacement from the original analysis data set. Parameter estimates obtained from the original dataset were compared with the median and 95% confidence intervals derived from a bootstrap based on 1000 replicated data sets.

Drug exposure derivation

The final population PK model was used to derive individual PK parameters. Maximum concentration at steady state ($C_{\max,ss}$), C_{\max} at first AE, AUC at steady-state during

the dosing interval ($AUC_{ss,tau}$) and AUC_{tau} at first AE were derived from noncompartmental analysis applied to concentration simulated at steady state or at first AE using the final population PK model, by considering individual PK primary parameters and by applying simulation time steps (0, 0.5, 1, 1.5, 2.5, 5.5, 12, 24, 48, 72, 96 to 144, 192, 240, 288, 336, 384, 432, 480, and 504 h). The dosing interval (τ) could be once every 2 or 3 weeks, depending on the study. Average concentration (C_{avg}) was calculated as the ratio between $AUC_{ss,tau}$ or AUC_{tau} at first AE and the relative dosing interval (τ). These parameters were then used for the exposure–safety analyses.

Exposure–safety analyses

Logistic regression analyses were conducted to assess the relationship between exposure and the two safety end points, diarrhea (grade ≥ 3) and neutropenia AEs (grade ≥ 3), for all patients receiving liposomal irinotecan-based regimens, in the NAPOLI-1 trial and the phase I/II 1L mPDAC trial. Neutropenia AEs were defined as neutropenia, decreased neutrophil count, and febrile neutropenia (umbrella approach). Only the earliest event (if any) for each patient and each endpoint was reported in the logistic regression analysis data set. Both data sets were then enriched with all the covariates included in the population PK data set.

The relationships between C_{avg} at steady state ($C_{avg,ss}$) or C_{avg} at first AE for total irinotecan and SN-38 and the probability of diarrhea (grade ≥ 3) and neutropenia AEs (grade ≥ 3) at first event were assessed with the logistic regression models and the `glm` function in R, as performed in a previous analysis.¹⁷ The alternative exposure parameters ($C_{max,ss}$ or C_{max} at first AE) were also considered. Logistic regression models were each time applied to exposure metrics or log-transformed exposure metrics in order to improve handling of a wide number of exposure metrics.

RESULTS

Observed data

For the PK analysis, data were available for a total of 440 patients from seven studies (Table 1). These patients received liposomal irinotecan at dose regimens ranging from 35 mg/m² free base (40 mg/m² irinotecan hydrochloride trihydrate) every 2 weeks to 156 mg/m² free base (180 mg/m² irinotecan hydrochloride trihydrate) every 3 weeks. Overall, 51% (226/440) of patients were men and 35% (154/440) of patients were Asian. The incidence of the UGT1A1*28 homozygous 7/7 genotype was 6.1% across all studies.

Overall, there were 5735 observations: 2879 for total irinotecan and 2856 for SN-38, of which 23% and 25% of values, respectively, were below the LLOQ; 16 observations (9 for total irinotecan and 7 for SN-38) corresponded to unexpected quantifiable predose levels and were excluded. The remaining 1887 and 1827 observations for total irinotecan and SN-38, respectively, were included in the population PK model. Exploratory plots of total irinotecan and SN-38 plasma concentration–time profiles normalized by actual doses are presented by study in Figure S1.

Population PK model and derived parameters

Initially, irinotecan alone (molar unit) was modeled to identify the best base structural model between two and three compartments: a two-compartment structural model was more stable and was statistically more significant than a three-compartment model. A joint model of irinotecan and SN-38 (both in molar units) was explored assuming two compartments for irinotecan and exploring whether one or two compartments were needed for SN-38. One compartment was selected for SN-38. Several approaches were implemented to try to capture the multiple peaks in SN-38. The Adiwijaya model,¹⁵ which added an impurity term to account for the quick peak in the SN-38 profile, was investigated without success, affecting the structural model of irinotecan. An enterohepatic recycling model and a model fixing the fraction of irinotecan converted to SN-38 (0.15)³¹ were tested but both had poor fitting and parameter estimates. The final population PK model for total irinotecan after administration of liposomal irinotecan comprised two compartments for irinotecan and one compartment for SN-38, with linear transformation of parent to metabolite through two metabolic pathways: one direct with a first-order constant from the central compartment of irinotecan (9%) and one delayed via a transit compartment (35%; Figure 1). Considering M3 methods with the base model (without covariates), no impact on goodness-of-fit plots and parameter estimates were observed except a large increase in relative standard errors and model instability compared with the M1 method (i.e., a lower rate of successful minimizations and covariance steps). Additional VPCs for the model using the M3 method were performed by considering the proportion of BLOQ samples. Because LLOQ values differed between studies, VPCs were split by LLOQ values. For irinotecan, considering the highest LLOQ value (1 $\mu\text{g/mL}$), the proportion of predicted BLOQ samples was higher than the observed number of BLOQ samples (Figure S2). A table comparing the base model with M1 and M3 methods

is provided in the Supplementary Material (Table S2). Owing to the large residual standard error (RSE; >1000%) obtained with the run using the M3 method, no statistical differences were found for all fixed parameters (except for total irinotecan clearance [CLP]). The high RSE values of the distribution parameters for irinotecan obtained with the M3 method suggested that irinotecan should be defined by one compartment. However, this is not aligned with the two compartments found when irinotecan data were first analyzed, or with data reported in the literature.³¹ Thus, owing to the lack of accuracy of estimates in NONMEM (even after trying several reruns by changing initial estimates using the “retries” function in Psn), it was decided to continue covariate model building (stepwise covariate modeling process) without retaining BLOQ samples by applying the M1 method.

Total irinotecan clearance was estimated at 17.9 L/week and was 20% higher in Asian patients than in individuals of other ethnicities (Table 2). Central and peripheral volumes of distribution were 4.09 L and 0.421 L, respectively, and distribution of the total irinotecan volume increased with increasing body surface area. Clearance of SN-38 was estimated to be 19,800 L/week; high bilirubin levels were associated with low SN-38 clearance. Clearances of both total irinotecan and SN-38 were 20% lower in women than in men. Co-administration of oxaliplatin was associated with an increase in clearance of total irinotecan of ~34% and a decrease of equivalent magnitude in clearance of SN-38. Drug manufacturing site (previous site vs. current site) was associated with a 37.6% increase in the fraction of liposomal irinotecan elimination feeding the

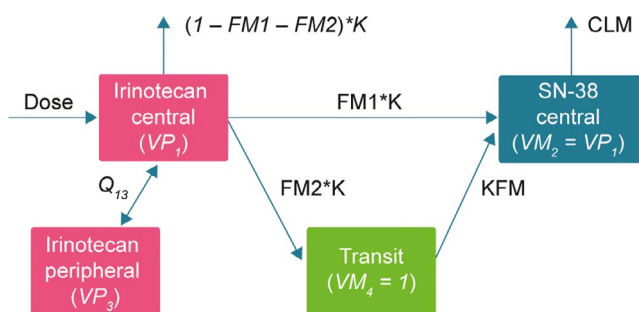


FIGURE 1 Structural population PK model for irinotecan and SN-38 after administration of liposomal irinotecan. CLM, SN-38 clearance; K, irinotecan total clearance/irinotecan central volume; FM1, fraction of irinotecan metabolized via first-order process; FM1*K, fraction of total clearance to SN-38 (first-order); FM2, fraction of irinotecan metabolized via transit; FM2*K, fraction of total clearance to SN-38 (transit); $(1 - FM1 - FM2)*K$, fraction of total clearance not transformed to SN-38; KFM, rate of transformation after delay; PK, pharmacokinetic; Q_{13} , inter-compartmental clearance; VP_1 , irinotecan central volume; VP_3 , irinotecan peripheral volume; VM_2 , SN-38 central volume (fixed to VP_1); VM_4 , transit compartment

transit compartment, a 12.8% decrease in irinotecan central volume of distribution, and a 51.5% increase in irinotecan total elimination clearance. Liposomal irinotecan manufactured at the previous site was used in phase I studies conducted before 2012; liposomal irinotecan manufactured at the current site was used in all pivotal studies (e.g., NAPOLI-1 and phase I/II 1L mPDAC study).

There was no significant association between UGT1A1*28 polymorphism (homozygous 7/7 vs. others) and SN-38 clearance based on the LRT. Box plots of SN-38 clearance by UGT1A1*28 polymorphism (homozygous 7/7 and others) are shown in Figure 2. The final NONMEM code is available in Supplementary Materials.

Model evaluation

Goodness-of-fit plots for the final model were in line with expectations and confirmed the appropriateness of the selected model for both total irinotecan and SN-38 (Figure S3). Relative standard errors for all model parameters were below 50%, indicating good precision.

The pcVPCs were satisfactory for both total irinotecan and SN-38, and were considered to describe the variability well overall (Figure 3 and Figure S4) and by study (Figure S5). However, it appeared that the model did not properly describe the high concentrations of SN-38, mainly in the fifth percentile. Of the 1000 bootstrap runs, 721 minimized successfully; all parameter estimates from the model were consistent with the relative median values and fell within 95% confidence intervals of the bootstrap parameter estimates, indicating robustness and stability of the model (Table S3). Thus, the model was considered acceptable for its intended purpose, which was to predict exposures in patients with mPDAC for the exposure–safety analyses. Caution is required regarding the risk of underprediction of SN-38 C_{max} .

Exposure–safety analyses

The data set for exposure–safety analyses included 316 patients (260 from NAPOLI-1 and 56 from the phase I/II 1L mPDAC study) and 316 observations. For each safety parameter examined, no difference was found between $C_{max,ss}$ and C_{max} at first AE; the same was observed for C_{avg} as detailed in the Supplementary Material (Figures S6 and S7). Thus, only derived exposure metrics at steady state are presented in this analysis. Additional logistic regression plots are also provided in the Supplementary Material comparing exposure metrics and log-transformed exposure metrics (Figures S8–S15). The same conclusions were obtained from both approaches.

TABLE 2 Estimated population PK parameters from the final model

Parameter	Estimate	RSE, %	IIV (% CV)	RSE, % of variance
Irinotecan total clearance, L/week	17.9	5.14	0.545 (85.2)	11
Asian race ^a	1.204	44.6		
Manufacturing site ^a	1.515	27.9		
Gender ^a	0.799	23.5		
Oxaliplatin administration ^a	1.339	28.1		
Irinotecan central volume, L	4.09	2.23	0.066 (26.1)	27.5
Body surface area ^b	$(BSA/1.71)^{0.573}$	17.9		
Manufacturing site ^a	0.872	29.4		
Gender ^a	0.886	22.9		
Fraction of delayed irinotecan total rate of elimination	0.629	23.4	0.188 (45.4)	26.4
Manufacturing site ^a	1.376	41		
Fraction of direct irinotecan total rate of elimination	0.152	22.4	0.928 (124)	10.9
Irinotecan inter-compartmental clearance, L/week	1.35	28.6		
Irinotecan peripheral volume, L	0.421	22.6		
SN-38 total clearance, L/week	19,800	12.8	0.126 (36.6)	13.6
Bilirubin ^b	$(BIL/0.41)^{-0.266}$	17.5		
Creatinine clearance ^b	$(CrCL/85.04)^{0.25}$	28.7		
Gender ^a	0.802	20.3		
Oxaliplatin administration ^a	0.656	14.1		
Rate of transformation after delay, 1/week	2	5.1	0.135 (38)	29.1
Covariance (correlation) between irinotecan total clearance and fraction of direct transformation	-0.558 (-0.785)	12		
Covariance (correlation) between irinotecan total clearance and central volume	0.117 (0.617)	17.8		
Covariance (correlation) between irinotecan central volume and fraction of direct transformation	-0.103 (-0.416)	24.4		
Residual error				
Proportional error on irinotecan	0.243 (CV, 24.3%)	6.25		
Proportional error on SN-38	0.291 (CV, 29.1%)	5.23		
Correlation between irinotecan and SN-38 errors	0.323	26.4		

Abbreviations: BIL, bilirubin; BSA, body surface area; CrCL, creatinine clearance; CV, coefficient of variation; IIV, interindividual variability; PK, pharmacokinetic; RSE, relative standard error.

^aCategorical covariates

^bContinuous covariates: irinotecan total clearance, $i = 17.9 \times 1.204^{\text{Asian}} \times 1.515^{\text{Manufacturing site}} \times 0.799^{\text{Gender}} \times 1.339^{\text{Oxaliplatin coadministration}}$

irinotecan central volume, $i = 4.09 \times \left(\frac{BSA, i^{0.573}}{1.71}\right) \times 0.872^{\text{Manufacturing site}} \times 0.886^{\text{Gender}}$

fraction of delayed irinotecan total rate of elimination, $i = 0.629 \times 1.376^{\text{Manufacturing site}}$

fraction of direct irinotecan total rate of elimination, $i = 0.152$

irinotecan inter-compartmental clearance, $i = 1.35$

irinotecan peripheral volume, $i = 0.421$

SN-38 total clearance, $i = 19,800 \times \left(\frac{BIL, i^{-0.266}}{0.41}\right) \times \left(\frac{CrCL, i^{0.25}}{85.04}\right) \times 0.802^{\text{Gender}} \times 0.656^{\text{Oxaliplatin coadministration}}$

Diarrhea

Overall, 17.7% of patients experienced diarrhea AEs (grade ≥ 3) at first event (16.9% and 21.4% in the NAPOLI-1 and phase I/II 1L mPDAC studies, respectively).

There were statistically significant exposure-safety relationships between the log-transformed C_{avg} for both total irinotecan and SN-38 and the probability of diarrhea AEs (grade ≥ 3) at first event (odds ratio [OR] 8.70, $p = 0.001$ for total irinotecan; OR 7.30, $p = 0.013$ for

SN-38), with increasing exposure associated with increasing probability of an event (Figure 4). In equivalent exposure–safety analyses using C_{\max} , there was a

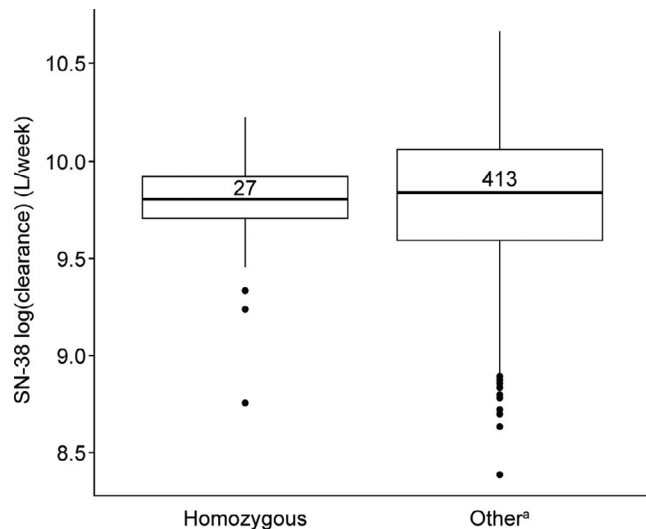


FIGURE 2 Impact of UGT1A1*28 homozygous 7/7 genotype on SN-38 clearance. Each box plot shows the median, interquartile range, and sample size. Outliers are represented by black circles.

^aHeterozygous 6/7, homozygous wild-type 6/6, and negative/unknown/missing genotypes

significant association between total irinotecan C_{\max} and the probability of diarrhea AEs (grade ≥ 3) at first event. However, the association between SN-38 C_{\max} and the probability of diarrhea AEs (grade ≥ 3) did not reach statistical significance.

Neutropenia AEs (neutropenia, decreased neutrophil count, and febrile neutropenia)

At least one neutropenia AE (grade ≥ 3) at first event was reported for 24.7% of patients overall and for 20.8% and 42.9% of patients from the NAPOLI-1 and phase I/II 1L mPDAC studies, respectively.

The probability of neutropenia AE (grade ≥ 3) at first event decreased with increasing exposure to total irinotecan, and the exposure–safety relationship was statistically significant (total irinotecan $\log_{10} C_{\text{avg}}$ as a predictor: OR 0.33, $p = 0.012$; Figure 5a). In the equivalent analysis for SN-38, there was no statistically significant exposure–safety relationship for neutropenia AE (grade ≥ 3) at first event (SN-38 $\log_{10} C_{\text{avg}}$ as a predictor: OR 3.14, $p = 0.115$; Figure 5b). The same analyses conducted with C_{\max} provided similar results.

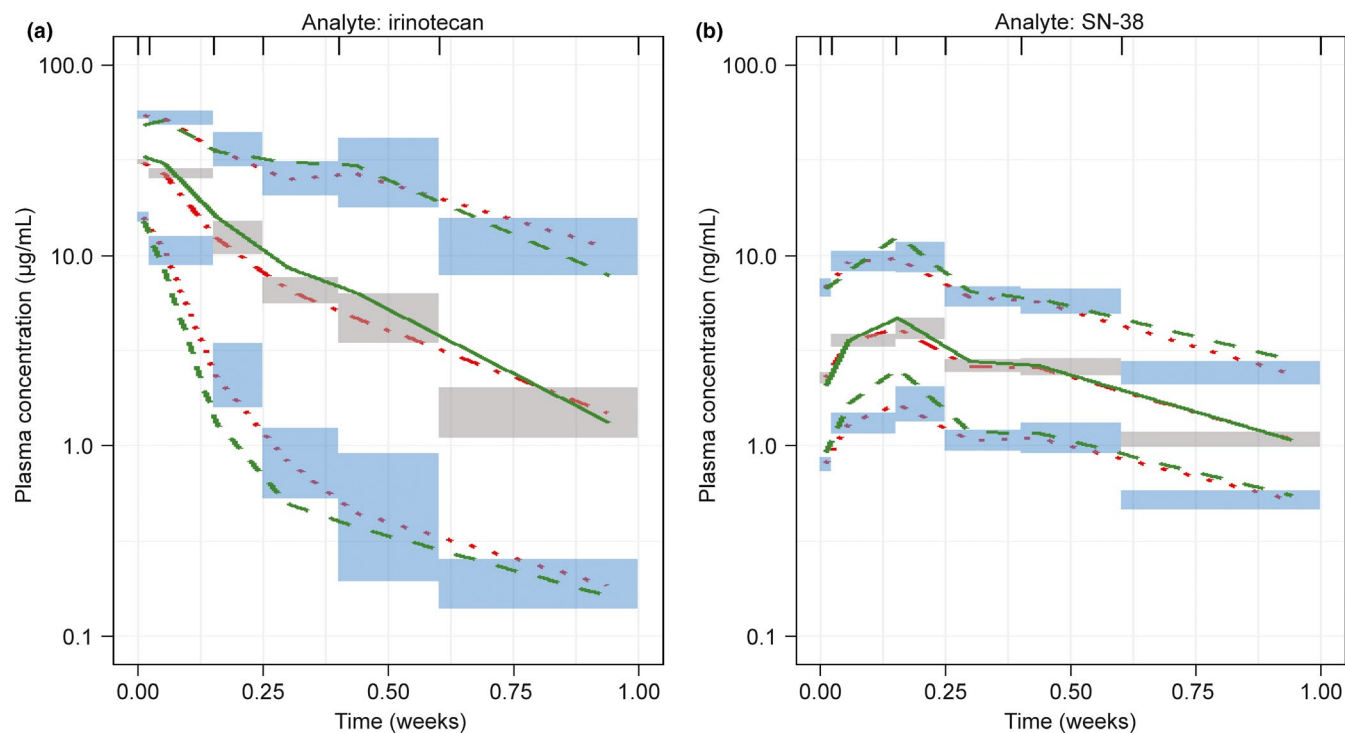
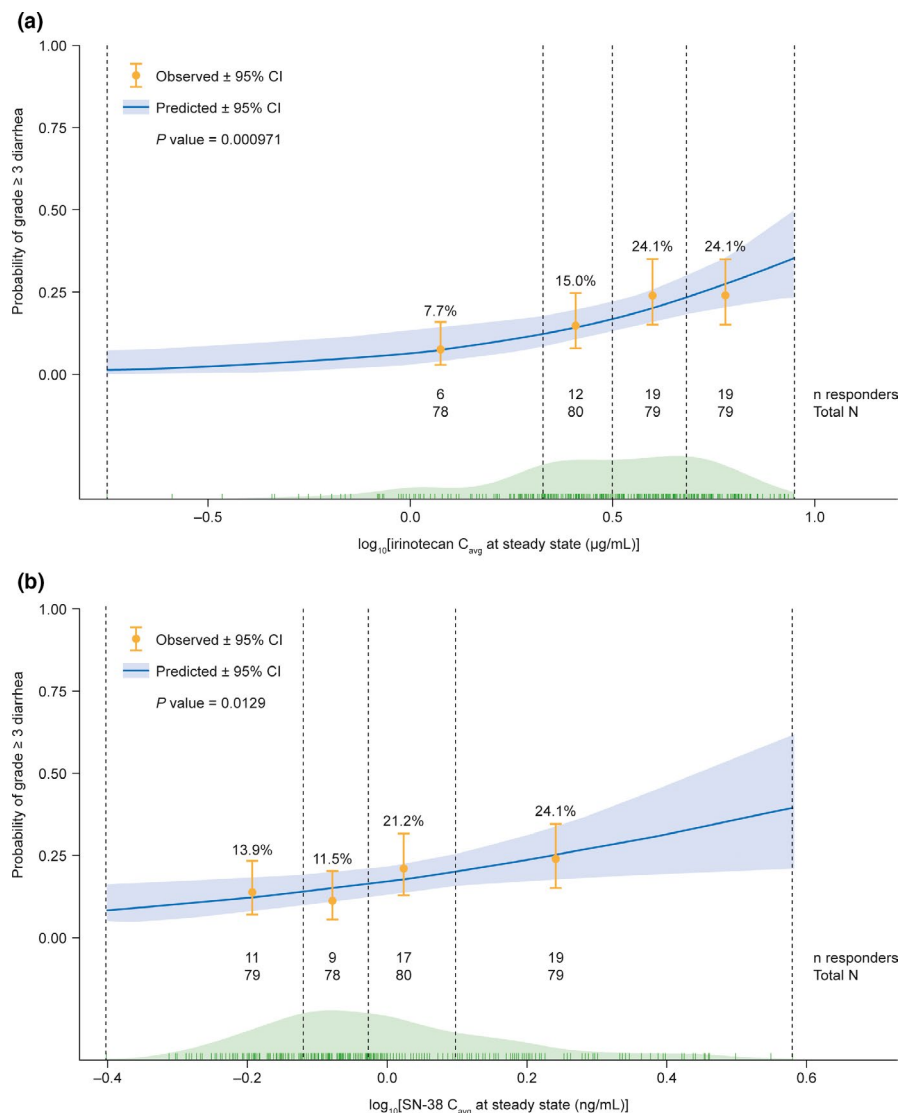


FIGURE 3 The pcVPCs for total irinotecan (a) and SN-38 (b) concentrations over time. Data are presented on a semi-log scale. The observed median (green bold line) and 2.5th and 97.5th percentiles (green dashed lines) are compared with the 95th confidence intervals (shaded area) for the median (gray area) and the 2.5th and 97.5th percentiles of the simulated ($n = 1000$) data (blue area). Simulated median (red semi-dashed line) and 2.5th and 97.5th simulated percentiles (red dotted line) are overlaid. pcVPC, prediction-corrected visual predictive check

FIGURE 4 Probability of developing diarrhea (grade ≥ 3) as a function of log-transformed $C_{avg,ss}$ for total irinotecan (a) and SN-38 (b) after administration of liposomal irinotecan. $C_{avg,ss}$, average plasma concentration at steady state; CI, confidence interval



DISCUSSION

The present analyses were performed to jointly characterize the PKs of total irinotecan and SN-38 after administration of liposomal irinotecan, and to understand the relationship between total irinotecan and SN-38 exposure and the incidence of key safety outcomes in patients with mPDAC.

The final population PK model appeared to be sufficiently robust to characterize the joint relationship between total irinotecan and SN-38, and therefore their relative exposures, in patients with mPDAC in the NAPOLI-1 and phase I/II 1L mPDAC trials. The overall model estimate for the total clearance of SN-38 was relatively high, at 118 L/h. This is probably a result of the lack of data supporting the estimate of the real volume of distribution for SN-38 and the prolonged elimination of irinotecan as a consequence of liposomal encapsulation. Thus, the true elimination of SN-38 is most likely masked by the prolonged release and metabolism of liposomal irinotecan, leading to formation rate-limited kinetics for SN-38.

The model developed in a previous analysis performed by Adiwijaya,¹⁵ which included 353 of the 440 patients included in the present model, was not selected as a starting model for the following reasons. Firstly, in the Adiwijaya model, irinotecan and SN-38 were developed independently (i.e., this was not a joint model) and only irinotecan clearance was included as a covariate in the SN-38 model. Non-joint models are not optimal for parent-metabolite model development (e.g., for testing drug-drug interactions, or for pediatric extrapolation). Second, the assumption of total versus unencapsulated SN-38 concentrations (with a fraction of encapsulated SN-38 measured in vitro of 0.015%) seems to be less meaningful than the assumption that 95% of irinotecan remains liposome-encapsulated during circulation when liposomal irinotecan is measured directly. Thus, the fraction of unencapsulated liposome could directly be metabolized in SN-38, which corresponds to the first order part of the final model developed here. This joint model also allows improved characterization of SN-38 clearance when SN-38 is obtained directly from the

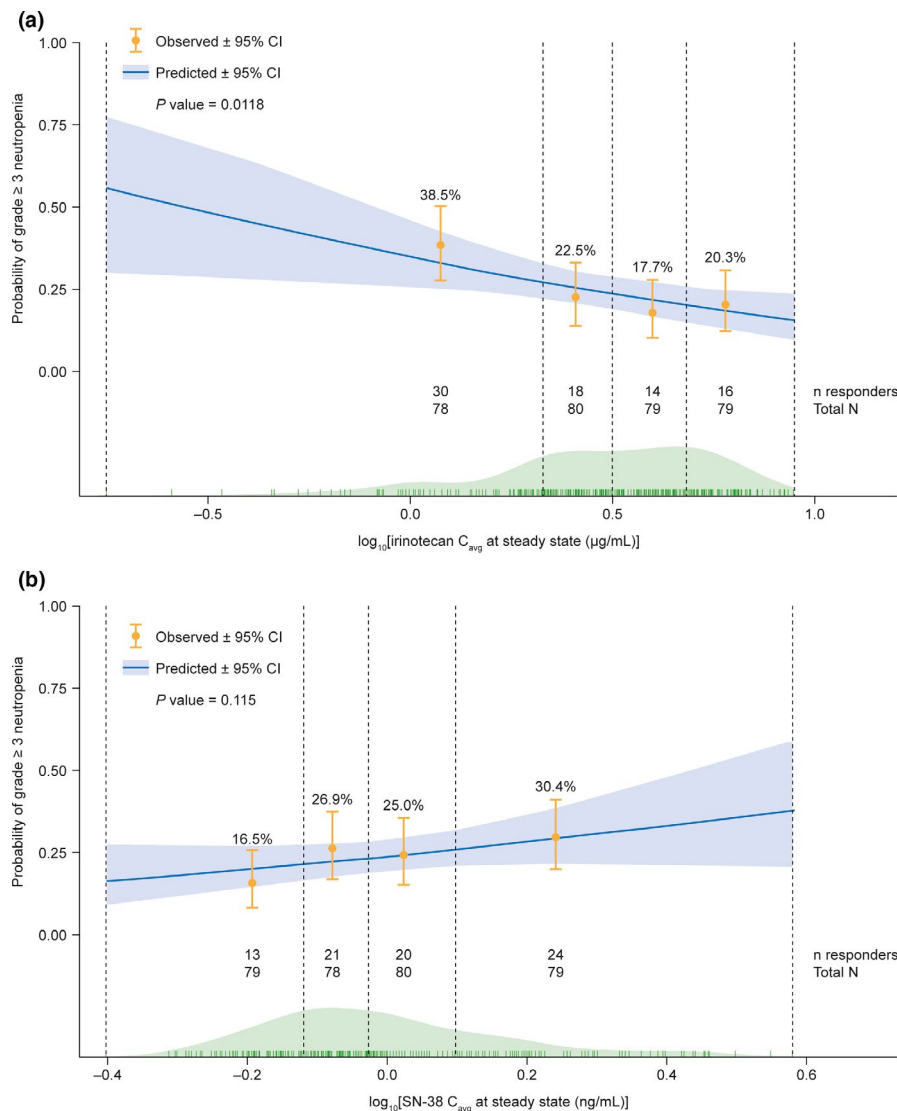


FIGURE 5 Probability of developing neutropenia AEs (grade ≥ 3) as a function of log-transformed $C_{avg,ss}$ for total irinotecan (a) and SN-38 (b) after administration of liposomal irinotecan. AE, adverse event; $C_{avg,ss}$, average plasma concentration at steady state; CI, confidence interval

fraction of unencapsulated liposome. Otherwise, SN-38 elimination coming from encapsulated irinotecan is driven by the rate of SN-38 formation.

Multiple covariates were incorporated into the model to test their role in the interpatient variability of PK exposures. The PK metrics affected by the largest number of covariates were total clearance of irinotecan and total clearance of SN-38. The 20% higher clearance of total irinotecan in Asian patients versus patients of other ethnicities is consistent with a previous report of lower levels of total irinotecan in Asian patients compared with White patients following administration of liposomal irinotecan.¹⁵ The covariates gender and co-administration of oxaliplatin affected clearance of both irinotecan and SN-38, although oxaliplatin administration was associated with an increase in clearance of total irinotecan and a decrease in clearance of SN-38. The lower clearances of irinotecan and SN-38 in women versus men after administration of liposomal irinotecan are consistent with previous reports of higher exposure of SN-38 in women after administration

of non-liposomal irinotecan.^{32,33} Given that liposomal formulation is complex, some manufacturing adjustments were performed between the previous manufacturing site (mainly dedicated to phase I studies) and the current site (used for all pivotal studies).

UGT1A1 is the key enzyme responsible for the inactivation of SN-38 via glucuronidation in the liver to form SN-38G, which is primarily eliminated by biliary excretion.⁶ The presence of the UGT1A1*28 allele has been reported to reduce expression of the UGT1A1 enzyme by 70%, leading to increased exposure to SN-38 and an increase in risk of irinotecan-related toxicity, most notably neutropenia and/or diarrhea (both grade ≥ 3).^{6,34,35} In the present analysis, there was no significant association between UGT1A1*28 polymorphism and SN-38 clearance, consistent with the finding in a previous analysis of liposomal irinotecan and SN-38 PK that UGT1A1*28 genotype was not a significant covariate to SN-38 clearance.¹⁵ A possible explanation for this is that the liposomal encapsulation slows the release of irinotecan and therefore reduces the load of SN-38,

such that the release of irinotecan is the rate-limiting step, and metabolism by UGT enzymes does not become saturated, even in patients with reduced UGT activities (e.g., UGT1A1*28 7/7 homozygous).¹⁵ It follows that patients with reduced UGT activities may not have higher SN-38 exposure. It should be noted that the limited number of patients with the UGT1A1*28 7/7 homozygous genotype and the lower starting dose of liposomal irinotecan (reduced by 20 mg/m²) in patients with this genotype in the NAPOLI-1 trial preclude firm conclusions from being drawn regarding the impact of this variable. Nevertheless, this analysis, which demonstrated that UGT1A1*28 status had no significant impact on the PKs of total irinotecan and SN-38 after administration of liposomal irinotecan-containing regimens, suggests that there is insufficient evidence of a need for dose adjustment based on UGT1A1*28 genotype. These results are also consistent with the decision tree for UGT1A1 genotyping depending initially on the dose of non-liposomal irinotecan (UGT1A1 genotyping not recommended for doses <180 mg/m² of irinotecan).³⁶

The sparse sampling design of the NAPOLI-1 study (cycle 1: 1.5, 2.5, 48, and 168 h), could affect the ability to estimate C_{max} , mainly for the metabolite SN-38. Lack of information from NAPOLI-1 could result in an underestimation of C_{max} compared with values obtained from studies with richer PK sampling designs.

Logistic regression analyses have demonstrated that both total irinotecan and SN-38 C_{avg} were significant predictors of diarrhea (grade ≥ 3), with the increase in probability of diarrhea AEs at first event explained as a function of increasing exposures. Irinotecan appeared to be a slightly stronger predictor than SN-38 based on the lower p value (0.001 vs. 0.013) and higher OR (8.70 vs. 7.30). Analyses using C_{max} were consistent with these results for total irinotecan, but no significant association was seen between SN-38 C_{max} and the probability of diarrhea AEs (grade ≥ 3). The results with C_{max} must be interpreted with caution, however, owing to the difficulty of reliably capturing the maximum exposures in the model.

There was no significant relationship between SN-38 C_{avg} and the probability of neutropenia AEs (grade ≥ 3). This absence of a relationship between SN-38 exposure and severe neutropenia could be explained by the difference in SN-38 PK profile between non-liposomal and liposomal irinotecan—the concentration profile is flatter for liposomal than for non-liposomal irinotecan. A link between SN-38 exposure and severe neutropenia has previously been demonstrated after administration of non-liposomal irinotecan³⁷; however, given that SN-38 PK profiles (including exposure) were deemed to be similar regardless of UGT1A1*28 status, no impact of SN-38 exposure on severe neutropenia is expected from UGT1A1*28 genotype status. The reduction in the probability of grade 3 neutropenia with

increasing exposure to total irinotecan was unexpected and further investigation will be performed in ongoing phase III studies (e.g., the effects of granulocyte colony stimulating factor supplementation on neutropenia will be evaluated).

Further investigations will be performed by updating the population PK model and exposure–safety assessment with new data from the ongoing phase III NAPOLI-3 trial (NCT04083235). This study will compare the efficacy and safety of 1L gemcitabine/nab-paclitaxel with NALIRIFOX in patients with mPDAC, using the doses established in the 1L PDAC phase I/II study. It is planned that 750 patients (375 in each arm) will be enrolled, which will allow improved understanding of the relationship between total irinotecan and/or SN-38 exposure and diarrhea and neutropenia AEs. In addition, a lower LLOQ for the analysis of both total irinotecan and SN-38 implemented during the NAPOLI-3 trial will allow for improved characterization of the terminal phase and lead to a more accurate determination of total clearance for both compounds.

In conclusion, the final population PK model appeared to be robust in characterizing the exposures of total irinotecan and SN-38 after administration of liposomal irinotecan. The results suggest that UGT1A1*28 status has no significant impact on the PK of liposomal irinotecan. In the exploratory exposure–safety analyses in patients with mPDAC, the risk of diarrhea (grade ≥ 3) was associated with both total irinotecan and SN-38 C_{avg} , but there was no significant association between an increased risk of neutropenia (grade ≥ 3) and SN-38 C_{avg} . In clinical practice, appropriate use of anti-diarrheal medication is an important factor when managing patients receiving irinotecan.³⁸

ACKNOWLEDGEMENTS

The authors thank all patients involved in the studies, as well as their caregivers, care teams, investigators, and research staff in participating institutions. The authors also thank Emma Bolton, DPhil, and Tamzin Gristwood, PhD, of Oxford PharmaGenesis, Oxford, UK, for providing editorial support, which was sponsored by Ipsen in accordance with Good Publication Practice guidelines. The authors thank Marta Neve of Certara for her contribution to the work.

CONFLICT OF INTEREST

K.B. is a full-/part-time employee of Ipsen. T.B.-S. has received advisory/consultancy fees from: 1Globe Health Institute, AbGenomics, Amgen, Array BioPharma, AstraZeneca, Bayer, Boehringer Ingelheim, Boston Biomedical, Bristol Myers Squibb, Celgene, Clovis Oncology, Eli Lilly, Exelixis, Genentech, Immuneering, Imugene, Incyte, Ipsen, Merck, Pancreatic Cancer Action Network (PanCAN), Seattle Genetics, Sobi, Sun BioPharma, Treos Bio. P.M.B. has received research grants/

funding from: Advaxis, Bayer, Boehringer Ingelheim, Boston Biomedical, Cascadian Therapeutics, Genentech, Merck; has received advisory/consultancy fees from: Bayer, Merrimack Pharmaceuticals; and honoraria from: Sirtex Medical. F.D. has received institutional research grants/funding from: Amgen, AstraZeneca, Bristol Myers Squibb, Exelixis, Ipsen, Taiho Pharmaceutical; has received advisory/consultancy fees from: Eisai, Exelixis, Foundation Medicine, Genentech, Ipsen, Natera (Signatera), QED Therapeutics; speaker bureau/expert testimony: Amgen, Deciphera Pharmaceuticals, Eisai, Exelixis, Ipsen, Natera (Signatera), Sirtex Medical; and their spouse/financial dependent is a full-/part-time employee of: Roche Diagnostics. A.D. has partaken in non-remunerated advisory/consultancy activities for: Shire, Specialised Therapeutics; and has received compensation for travel/accommodation/expenses from: Amgen. T.M. has received research grants/funding from: Agios, ASLAN Pharmaceuticals, AstraZeneca, Bayer, Biogen, Celgene, Eli Lilly, Genentech, Halozyme Therapeutics, Immunomedics, Merrimack Pharmaceuticals, Millennium Pharmaceuticals, Novartis, Novocure, OncoMed Pharmaceuticals, Pfizer, Pharmacyclics, Roche; has received fees from: Eli Lilly, Ipsen, Roche, Sanofi, Sanofi Genzyme, Shire, Tesaro; has received advisory/consultancy fees from: Baxalta, Celgene, H3 Biomedicine, Incyte, QED Therapeutics, Sanofi Genzyme, Servier, Shire; has provided speaker bureau/expert testimony for: Celgene, Sanofi, Shire; and has received compensation for travel/accommodation/expenses from: Bayer, H3 Biomedicine, Merck, Sanofi. F.M. is a full-/part-time employee and owner of shares/stocks/stock options of Ipsen. K.M. has received research grants/funding from: Agios, ArQule, AstraZeneca, Genentech, Incyte, National Cancer Institute of the National Institutes of Health award # NCI/NIH P50 CA210964, Puma Biotechnology, Senhwa Biosciences, Taiho Pharmaceutical; and has received advisory/consultancy fees from: AstraZeneca, Bayer, Celgene, Eisai, Exelixis, Ipsen, Merrimack Pharmaceuticals, Vicus Therapeutics. A.P.-D. is a full-/part-time employee of: Ipsen. Z.A.W. has received institutional research grants/funding from: Five Prime Therapeutics, Ipsen, Novartis, Plexxikon; and has received advisory/consultancy fees from: AstraZeneca, Bayer, Daiichi Sankyo, Eli Lilly, Five Prime Therapeutics, Ipsen, Merck, QED Therapeutics. B.Z. is a full-/part-time employee and owner of shares/stocks/stock options of Ipsen; and received licensing/royalties from Ipsen. Funding information: This study was sponsored by Ipsen.

AUTHOR CONTRIBUTIONS

K.B., T.B.-S., P.M.B., F.D., A.D., T.M., F.M., K.M., A.P.-D., Z.A.W., and B.Z. wrote the manuscript. K.B., F.M., A.P.-D., and B.Z. designed the research. K.B., T.B.-S., P.M.B., F.D.,

A.D., T.M., F.M., K.M., A.P.-D., Z.A.W., and B.Z. performed the research. K.B., T.B.-S., P.M.B., F.D., A.D., T.M., F.M., K.M., A.P.-D., Z.A.W., and B.Z. analyzed the data.

REFERENCES

1. Sohal DP, Walsh RM, Ramanathan RK, Khorana AA. Pancreatic adenocarcinoma: treating a systemic disease with systemic therapy. *J Natl Cancer Inst.* 2014;106:dju011.
2. Bray F, Ferlay J, Soerjomataram I, Siegel RL, Torre LA, Jemal A. Global cancer statistics 2018: GLOBOCAN estimates of incidence and mortality worldwide for 36 cancers in 185 countries. *CA Cancer J Clin.* 2018;68:394-424.
3. Ducreux M, Cuhna AS, Caramella C, et al. Cancer of the pancreas: ESMO Clinical Practice Guidelines for diagnosis, treatment and follow-up. *Ann Oncol.* 2015;26(suppl. 5):v56-v68.
4. National Comprehensive Cancer Network. Pancreatic adenocarcinoma, version 2.2021. 2020. https://www.nccn.org/professionals/physician_gls/pdf/pancreatic.pdf. Accessed May 2021.
5. ESMO Guidelines Committee. eUpdate – Cancer of the pancreas treatment recommendations. <https://www.esmo.org/guidelines/gastrointestinal-cancers/pancreatic-cancer/eupdate-cancer-of-the-pancreas-treatment-recommendations2>. Accessed May 2021.
6. Chang TC, Shiah HS, Yang CH, et al. Phase I study of nanoliposomal irinotecan (PEP02) in advanced solid tumor patients. *Cancer Chemother Pharmacol.* 2015;75:579-586.
7. Iyer L, King CD, Whittington PF, et al. Genetic predisposition to the metabolism of irinotecan (CPT-11). Role of uridine diphosphate glucuronosyltransferase isoform 1A1 in the glucuronidation of its active metabolite (SN-38) in human liver microsomes. *J Clin Invest.* 1998;101:847-854.
8. Kawato Y, Aonuma M, Hirota Y, Kuga H, Sato K. Intracellular roles of SN-38, a metabolite of the camptothecin derivative CPT-11, in the antitumor effect of CPT-11. *Cancer Res.* 1991;51:4187-4191.
9. Liu JY, Qu K, Sferruzza AD, Bender RA. Distribution of the UGT1A1*28 polymorphism in Caucasian and Asian populations in the US: a genomic analysis of 138 healthy individuals. *Anticancer Drugs.* 2007;18:693-696.
10. Iyer L, Das S, Janisch L, et al. UGT1A1*28 polymorphism as a determinant of irinotecan disposition and toxicity. *Pharmacogenomics J.* 2002;2:43-47.
11. Hoskins JM, Goldberg RM, Qu P, Ibrahim JG, McLeod HL. UGT1A1*28 genotype and irinotecan-induced neutropenia: dose matters. *J Natl Cancer Inst.* 2007;99:1290-1295.
12. Ando Y, Saka H, Ando M, et al. Polymorphisms of UDP-glucuronosyltransferase gene and irinotecan toxicity: a pharmacogenetic analysis. *Cancer Res.* 2000;60:6921-6926.
13. Innocenti F, Undevia SD, Iyer L, et al. Genetic variants in the UDP-glucuronosyltransferase 1A1 gene predict the risk of severe neutropenia of irinotecan. *J Clin Oncol.* 2004;22:1382-1388.
14. Drummond DC, Noble CO, Guo Z, Hong K, Park JW, Kirpotin DB. Development of a highly active nanoliposomal irinotecan using a novel intraliposomal stabilization strategy. *Cancer Res.* 2006;66:3271-3277.
15. Adiwijaya BS, Kim J, Lang I, et al. Population pharmacokinetics of liposomal irinotecan in patients with cancer. *Clin Pharmacol Ther.* 2017;102:997-1005.
16. Klinz SG, Leonard SC, Paz N, et al. DNA damage with liposomal irinotecan (nal-IRI) in pancreatic cancer xenografts:

- multimodal analysis of deposition characteristics. *J Clin Oncol*. 2018;36(suppl.):e16205.
17. Leonard SC, Paz N, Klinz SG, et al. Deposition characteristics and resulting DNA damage patterns of liposomal irinotecan (nal-IRI) in pancreatic cancer xenografts. *J Clin Oncol*. 2018;36(suppl.):335.
 18. Wang-Gillam A, Li C-P, Bodoky G, et al. Nanoliposomal irinotecan with fluorouracil and folinic acid in metastatic pancreatic cancer after previous gemcitabine-based therapy (NAPOLI-1): a global, randomised, open-label, phase 3 trial. *Lancet*. 2016;387:545-557.
 19. Wang-Gillam A, Hubner RA, Siveke JT, et al. NAPOLI-1 phase 3 study of liposomal irinotecan in metastatic pancreatic cancer: final overall survival analysis and characteristics of long-term survivors. *Eur J Cancer*. 2019;108:78-87.
 20. Wainberg ZA, Bekaii-Saab T, Boland PM, et al. First-line liposomal irinotecan with oxaliplatin, 5-fluorouracil and leucovorin (NALIRIFOX) in pancreatic ductal adenocarcinoma: A phase I/II study. *Eur J Cancer*. 2021;151:14-24.
 21. Chiang NJ, Chao T-Y, Hsieh R-K, et al. A phase I dose-escalation study of PEP02 (irinotecan liposome injection) in combination with 5-fluorouracil and leucovorin in advanced solid tumors. *BMC Cancer*. 2016;16:907.
 22. Roy AC, Park SR, Cunningham D, et al. A randomized phase II study of PEP02 (MM-398), irinotecan or docetaxel as a second-line therapy in patients with locally advanced or metastatic gastric or gastro-oesophageal junction adenocarcinoma. *Ann Oncol*. 2013;24:1567-1573.
 23. Chen LT, Shiah H-S, Lin P-C, et al. Phase I study of biweekly liposome irinotecan (PEP02, MM-398) in metastatic colorectal cancer failed on first-line oxaliplatin-based chemotherapy. *J Clin Oncol*. 2012;30:613.
 24. Ipsen Pharmaceuticals Inc. MM-398 (nanoliposomal irinotecan, Nal-IRI) to determine tumor drug levels and to evaluate the feasibility of ferumoxytol magnetic resonance imaging to measure tumor associated macrophages and to predict patient response to treatment (NCT01770353). 2019. <https://clinicaltrials.gov/ct2/show/study/NCT01770353>. Accessed May 2021.
 25. Wainberg Z, Boland P, Lieu C, et al. SO-005. A phase 1/2, open-label, dose-expansion study of liposomal irinotecan (nal-IRI) plus 5-fluorouracil/leucovorin (5-FU/LV) and oxaliplatin (OX) in patients with previously untreated metastatic pancreatic cancer. *Ann Oncol*. 2019;30(suppl. 4):mdz157.004.
 26. Beal SL. Ways to fit a PK model with some data below the quantification limit. *J Pharmacokinet Pharmacodyn*. 2001;28:481-504.
 27. Ahn JE, Karlsson MO, Dunne A, Ludden TM. Likelihood based approaches to handling data below the quantification limit using NONMEM VI. *J Pharmacokinet Pharmacodyn*. 2008;35:401-421.
 28. Committee for Medicinal Products for Human Use (CHMP) Guideline on reporting results of population pharmacokinetic analyses. 2007. https://www.ema.europa.eu/en/documents/scientific-guideline/guideline-reporting-results-population-pharmacokinetic-analyses_en.pdf. Accessed May 2021.
 29. US Department of Health, H.S.F., Drug Administration Center for Drug Evaluation and Research (CDER). Guidance for industry, population pharmacokinetic analyses. 2019. <https://www.fda.gov/media/128793/download>. Accessed May 2021.
 30. Bergstrand M, Hooker AC, Wallin JE, Karlsson MO. Prediction-corrected visual predictive checks for diagnosing nonlinear mixed-effects models. *AAPS J*. 2011;13:143-151.
 31. Deyme L, Barbolosi D, Gattacceca F. Population pharmacokinetics of FOLFIRINOX: a review of studies and parameters. *Cancer Chemother Pharmacol*. 2019;83:27-42.
 32. Klein CE, Gupta E, Reid JM, et al. Population pharmacokinetic model for irinotecan and two of its metabolites, SN-38 and SN-38 glucuronide. *Clin Pharmacol Ther*. 2002;72:638-647.
 33. Slatter JG, Schaaf LJ, Sams JP, et al. Pharmacokinetics, metabolism, and excretion of irinotecan (CPT-11) following I.V. infusion of [(14)C]CPT-11 in cancer patients. *Drug Metab Dispos*. 2000;28:423-433.
 34. Bosma PJ, Chowdhury JR, Bakker C, et al. The genetic basis of the reduced expression of bilirubin UDP-glucuronosyltransferase 1 in Gilbert's syndrome. *N Engl J Med*. 1995;333:1171-1175.
 35. Palomaki GE, Bradley LA, Douglas MP, Kolor K, Dotson WD. Can UGT1A1 genotyping reduce morbidity and mortality in patients with metastatic colorectal cancer treated with irinotecan? An evidence-based review. *Genet Med*. 2009;11:21-34.
 36. Etienne-Grimaldi M-C, Boyer JC, Thomas F, et al. UGT1A1 genotype and irinotecan therapy: general review and implementation in routine practice. *Fundam Clin Pharmacol*. 2015;29:219-237.
 37. Ramchandani RP, Wang Y, Booth BP, et al. The role of SN-38 exposure, UGT1A1*28 polymorphism, and baseline bilirubin level in predicting severe irinotecan toxicity. *J Clin Pharmacol*. 2007;47:78-86.
 38. Bossi P, Antonuzzo A, Cherny N, et al. Diarrhoea in adult cancer patients: ESMO Clinical Practice Guidelines. *Ann Oncol*. 2018;29:iv126-iv142.

SUPPORTING INFORMATION

Additional supporting information may be found in the online version of the article at the publisher's website.

How to cite this article: Brendel K, Bekaii-Saab T, Boland PM, et al. Population pharmacokinetics of liposomal irinotecan in patients with cancer and exposure-safety analyses in patients with metastatic pancreatic cancer. *CPT Pharmacometrics Syst Pharmacol*. 2021;10:1550-1563. doi:[10.1002/psp4.12725](https://doi.org/10.1002/psp4.12725)